A model electronic structure for metal-intercalated zeolites

1995 J. Phys.: Condens. Matter 7 5507

(http://iopscience.iop.org/0953-8984/7/28/008)

J. Phys.: Condens. Matter 7 (1995) 5507–5519. Printed in the UK

A model electronic structure for metal-intercalated zeolites

M J Kelly
Department of Physics, University of Surrey, Guildford GU2 5XH, UK

Received 27 February 1995, in final form 24 April 1995

Abstract. We obtain the electronic structure of a simple model for zeolites which have been intercalated with metals, from which we can account for aspects of their electrical and optical properties. The results are reviewed in the context of a search for a dense bundle of quasi-one-dimensional wires.

1. Introduction

Much new physics has been discovered in reduced-dimensionality electronic systems over the last three decades, and some of this physics has been applied in electronic and optoelectronic devices [1]. The quasi two-dimensional (Q2D) electron gas at a semiconductor interface has been exploited in silicon MOSFETs and in high-electron mobility transistors. Quantum confinement of electrons and holes in thin layers has been exploited in laser structures. There have been many investigations of ballistic carrier phenomena in quasi-one-dimensional (Q1D) structures and few carrier effects in quasi-zero-dimensional (Q0D) structures. These remain to be exploited practically. One intrinsic problem, among many, in having Q1D or Q0D structures perform useful functions [2] is the statistical fluctuation associated both with the size of the small structures *per se* and with the small numbers of carriers involved in each structure.

The next move is towards three-dimensional structures that are made up of arrays of reduced dimensionality subunits. For a simple example of what is sought, see the appendix. The problem of few carriers will be eliminated by averaging over the large number of subunits, while individual carriers exploit the advantages of low dimensionality, such as a reduced phase space for scattering, or a narrower energy spread in the density of states. The rich variety of zeolite (alumino–silicate) minerals lend themselves to this programme [3]. These materials consist of a strongly-bonded and insulating silicate lattice which supports voids or columns of nanometre lateral dimensions, the latter extending through the entire crystal in one or more spatial dimensions (see figure 1 for a schematic diagram). When used for ion exchange as in water softening, the columns take up and transport water and ions. In the interests of forming a dense bundle of one-dimensional wires, it is proposed to take a uniaxial columnar structure and fill the columns with metallic elements.

By subjecting the minerals to high pressures and temperatures in the presence of low-melting point metals, it has been possible to force the metal into zeolite columns. So far Tl, Pb, Bi and most recently K have been used [4, 5]. The detailed stoichiometry of the former composite materials is not known, and so the integrity of the Q1D metallic wires is uncertain. In particular, if metal is absent from one or two unit cells of a given column we have an open circuit and no conduction in that column. One would need to rely on some communication between columns. Very anisotropic optical absorption throughout the visible

0953-8984/95/285507+13$19.50

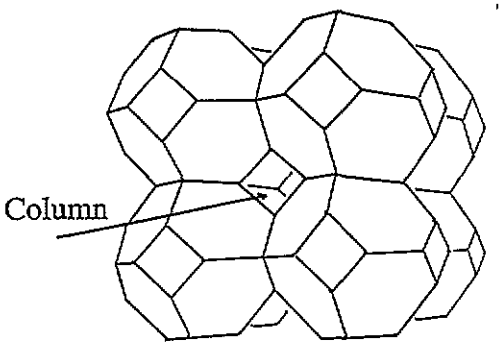

Figure 1. The unit cell of a typical zeolite structure, showing the rigid silicate cage, and the voids that can connect between adjacent unit cells to form columns. There are many variants on this structure that allow for columns in one or more spatial direction.

spectrum has been obtained consistent with the Q1D character of the wires [4]. Electron spin resonance of the potassium-intercalated zeolite shows that there is approximately one potassium-atom silicate per unit cell, and each atom provides one free electron: the white zeolite turns blue after intercalation, and there is indirect evidence of some anisotropy [5]. The density of intercalated atoms can be increased more than ten-fold over this value (P P Edwards and P Anderson, private communication). For completeness, we note that chains of selenium atoms have been intercalated into zeolites and their optical properties investigated [6].

In this paper we set up a simple model for the electronic structure of a dense bundle of Q1D wires appropriate to metal-intercalated zeolites. We calculate the density of states, conductivity and optical absorption within this model to establish the degree of anisotropy that might be anticipated. This turns out to be relatively modest but tailorable. We compare with the data available. We suggest further experiments and refinements to the theory. This exercise parallels an earlier one, where comparable properties were obtained for a certain type of tuneable Q2D electron gas [7], and subsequently verified [8].

2. The tight-binding-free-electron model electronic structure

2.1. Density of states

The simplest model is to consider our intercalated zeolite as a set of parallel conducting cylinders of radius a at a centre-to-centre distance, d. The two-dimensional crystal represented by a plane cross-section of the zeolite normal to the cylinder axis is a simple square lattice. This is a fair approximation (with $a \sim 0.34$ nm and $d \sim 2.0$ nm) to the case of the natural zeolite mordenite M, intercalated with Pb, Tl and Bi. In practice, we allow for a weak interaction between adjacent cylinders, so that the electronic structure is free-electron like in the direction of the cylinders, and tight-binding in the perpendicular direction. (In the next section, we include the fact that the cylinders are not straight-sided, but rather have a concertina-like cross-section, and we model this by the addition of a periodic potential (assumed weak) along the axis of the wire. This is important for the optical response.)

The energy band structure is modelled by ($\hbar$ =Planck's constant/2π)

$$E(k) = -2h(\cos k_x d + \cos k_y d) + \hbar^2 k_z^2/2m^* \tag{1}$$

where the relative energy scales parallel and perpendicular to the wires are set by m^*, the effective mass of motion along the wire, and the tight-binding parameter, $h > 0$, is the measure of the interaction energy between electrons in one wire and the one-electron potential in an adjacent wire. (We shall discuss the most appropriate values of these quantities below.) This simple model allows the density of states and conductivity to be obtained semi-analytically, i.e. the expressions are reduced to a single integral over analytic functions. The minimum energy is $-4h$ (when $\boldsymbol{k} = \boldsymbol{0}$), and in figure 2, one quadrant of the $k_z = 0$ section of the Brillouin zone is shown. Constant energy contours are shown with Fermi line in the lower left triangle for $-4h < E < 0$, and in the upper right for $0 < E < 4h$. The density of states per unit volume becomes an integral over the Brillouin zone, in this case $|k_x d| < \pi$, $|k_y d| < \pi$, and over all k_z

$$N(E) = \int \mathrm{d}\boldsymbol{k}/\delta(E - E(\boldsymbol{k}))(4\pi^3). \tag{2}$$

If we define

$$\Phi = E + 2h(\cos k_x d + \cos k_y d)$$

then

$$N(E) = (1/4\pi^3) \int \mathrm{d}k_x \int \mathrm{d}k_y \int \mathrm{d}k_z\, \delta(\Phi - \hbar^2 k_z^2/2m^*)$$

and with $\phi = k_x d$ and $\theta = k_y d$, we proceed to evaluate the density of states as four times the integral over the first (ϕ, θ) quadrant

$$N(E) = (1/d^2\pi^3) \int_0^\pi \mathrm{d}\phi \int_0^\pi \mathrm{d}\theta \sqrt{(2m^*/\hbar^2)\sqrt{(E + 2h(\cos\phi + \cos\theta))}}$$

provided $[E + 2h(\cos\phi + \cos\theta)] \geqslant 0$. For a given E such that $-4h < E < 0$, and for a given ϕ, there exists a θ^* such that $[E + 2h(\cos\phi + \cos\theta^*)] = 0$, and for each E there is a ϕ^* such that when $\theta = 0$ we have $[E + 2h(\cos\phi^* + 1)] = 0$. These quantities are shown in figure 2. In the case where $0 < E < 4h$, the corresponding terms are ϕ^* and θ^*. In each case, the θ integration can be performed analytically, leaving only the ϕ integration to be performed numerically. Using the definitions $\alpha(\phi) = E + 2h\cos\phi$ and $\beta = 2h$, the results are given in terms of integrals over the complete elliptic integrals of the first kind [9–12] $F(\pi/2, m)$

(i) $-4h < E < 0$

$$N(E) = (1/d^2\pi^3)\sqrt{(2m^*/\hbar^2)} \int_0^{\phi^*} \mathrm{d}\phi \int_0^{\theta^*} \mathrm{d}\theta/\sqrt{(\alpha(\phi) + \beta\cos\theta)}$$

$$= (1/d^2\pi^3)\sqrt{(2m^*/\hbar^2)} \int_0^{\phi^*} \mathrm{d}\phi\, \sqrt{(2/\beta)} F(\pi/2, \sqrt{((\alpha + \beta)/2\beta)})$$

(ii) $0 < E < 4h$

$$N(E) = (1/d^2\pi^3)\sqrt{(2m^*/\hbar^2)}\left(\int_0^{\phi^*} \mathrm{d}\phi \int_0^{\pi} \mathrm{d}\theta/\sqrt{(\alpha(\phi) + \beta\cos\theta)} \right.$$

$$\left. + \int_{\phi^*}^{\pi} \mathrm{d}\phi \int_0^{\theta^*} \mathrm{d}\theta/\sqrt{(\alpha(\phi) + \beta\cos\theta)} \right)$$

$$= (1/d^2\pi^3)\sqrt{(2m^*/\hbar^2)}\left(\int_0^{\phi^*} \mathrm{d}\phi\, (2/\sqrt{(\alpha + \beta)}) F(\pi/2, \sqrt{(2\beta/(\alpha + \beta))}) \right.$$

$$\left. + \int_{\phi^*}^{\pi} \mathrm{d}\phi\, \sqrt{(2/\beta)} F(\pi/2, \sqrt{((\alpha + \beta)/2\beta)}) \right)$$

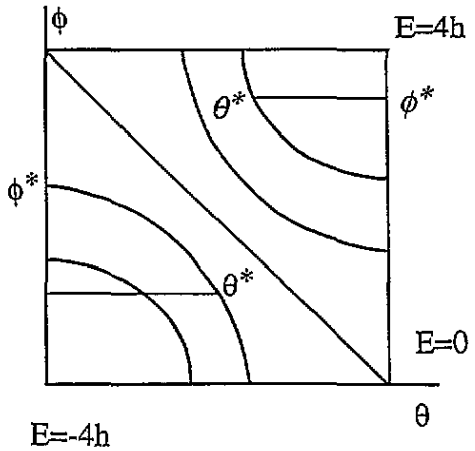

Figure 2. The energy contours in the $\phi = k_x d$ and $\theta = k_y d$ plane as used in calculating the density of states and conductivity. The significance of the θ^* and ϕ^* quantities are described in the text.

(iii) $E > 4h$

$$N(E) = (1/d^2\pi^3)\sqrt{(2m^*/\hbar^2)} \int_0^\pi d\phi \int_0^\pi d\theta/\sqrt{(\alpha(\phi) + \beta\cos\theta)}$$

$$= (1/d^2\pi^3)\sqrt{(2m^*/\hbar^2)} \int_0^\pi d\phi\, (2/\sqrt{(\alpha+\beta)}F(\pi/2, \sqrt{(2\beta/(\alpha+\beta))}).$$

In figure 3, we show the density of states in energy. Note the three dimensional character at low energy giving over to a quasi-one-dimensional $(1/\sqrt{E})$ form at higher energies ($> 4h$). The width of the peak is set solely by the two-dimensional tight-binding character, while the magnitude of the density of states also scales as $\sqrt{m^*}$. The position of the Fermi energy (E_f) is determined by the number of electrons per unit volume, and its position also depends on the size of the tight-binding parameter h. In the K-intercalated material [5] there is one electron per formula unit of zeolite (i.e. in a volume d^3). The position of E_f is marked in figure 3 for three cases, all having $m^* = m_e$ as is expected for Q1D alkali metals. The difference between $h = 3$ meV (i.e. a very narrow band) and $h = 100$ meV is in the relative energy dispersions in the directions perpendicular and parallel to the axis of the wires. The former has a 1D-like character for the density of states at E_f, the latter a 3D-like character.

2.2. *Estimated values of band structure parameters*

The most appropriate value for h is subject to some approximation. Using J_0/K_0 Bessel functions as the radial solutions $R(r)$ for the lowest energy wavefunctions inside/outside the cylinders of radius a, the expression for h (with $r = |\boldsymbol{r}|$, and $\boldsymbol{d}$ a vector of length d) is the one-electron potential $V(\boldsymbol{r})$, weighted by the overlap of the wavefunctions in adjacent wells

$$h = \int R(|\boldsymbol{r} - \boldsymbol{d}|)R(r)V(\boldsymbol{r})r\,dr\,d\theta. \tag{3}$$

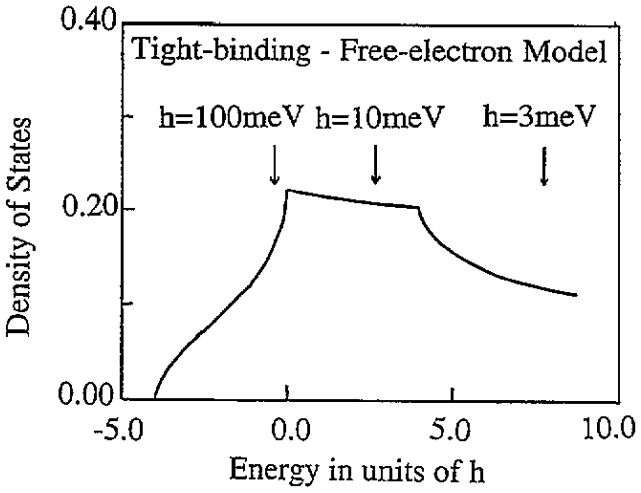

Figure 3. The density of states in energy (expressed in units of the parameter h) for the simple free-electron tight-binding band structure.

We approximate the one-electron potential as an array of finite-depth cylindrical wells of constant depth $-V_0$, with a constant interstitial potential $-V_1$. We obtain V_0 as the bottom of the conduction band in bulk potassium (work function + bulk Fermi energy = 4.34 eV), and we calculate the zero of energy in equation (1) from the first bound state of electrons in a cylinder of radius a ($E_0 \sim 1.75$ eV above $-V_0$ for $a = 0.35$ nm, if the well were infinitely deep, but only a third of this value if the well is only twice as deep as this first bound state). The value of the interstitial potential is estimated from a calculation of the overlap integral in the regime where $(V_1 - V_0) \sim 2E_0$ which gives $h \sim 0.1V_1$. The relevant value of V_1 is consistent with energies near the top of silica valence bands. If the potential well is much deeper, the value of h decreases rapidly. It is therefore likely in practice that $h \sim 0.05$–0.25 eV, i.e. a regime where there is likely to be significant 3D dispersion.

2.3. Conductivity

The corresponding expression for the conductivity in the relaxation time approximation is, as a function of the Fermi energy,

$$\sigma_{ij} = (e^2\tau/2\pi^2)\int_{\text{occupied bands}} \mathrm{d}k\,(1/\hbar^2)\,\mathrm{d}^2E(k)/\mathrm{d}k_i\,\mathrm{d}k_j$$

from the form of the energy bands, the conductivity is diagonal, and $\sigma_{xx} = \sigma_{yy}$. Here, τ is a phenomenological relaxation time: we return to the anisotropy of τ below. For convenience, we define a tight-binding mass $1/m^\dagger = 2hd^2/\hbar^2$. The same manipulations as above for the density of states give rise to an expression

$$\sigma = (4e^2\tau/(\pi^2d^2))\sqrt{(2m^*/\hbar^2)}\begin{pmatrix} J_1m^\dagger & 0 & 0 \\ 0 & J_{10}/m^\dagger & 0 \\ 0 & 0 & J_0/m^* \end{pmatrix}$$

where the J integrals are defined as

(i) $-4h < E < 0$

$$J_1 = \int_0^{\phi^*} I_1(\phi)\,\mathrm{d}\phi \qquad J_{10} = \int_0^{\phi^*} \cos(\phi) I_0(\phi)\,\mathrm{d}\phi \qquad \text{and} \qquad J_0 = \int_0^{\phi^*} I_0(\phi)\,\mathrm{d}\phi$$

with $I_0(\phi) = \sqrt{(2/\beta)}((\alpha-\beta)F(\pi/2, \sqrt{((\alpha+\beta)/2\beta)}) + 2\beta E(\pi/2, \sqrt{((\alpha+\beta)/2\beta)})$ and $I_1(\phi) = \sqrt{(2/\beta)}((\beta-\alpha)F(\pi/2, \sqrt{((\alpha+\beta)/2\beta)})/3 - 2\alpha E(\pi/2, \sqrt{((\alpha+\beta)/2\beta)})/3)$ where F and E and the complete elliptic integrals of the first and second kind respectively, and

(ii) $0 < E < 4h$

$$J_1 = \int_0^{\phi^*} I_1(\phi)\,\mathrm{d}\phi + \int_{\phi^*}^{\pi} I_1(\phi)\,\mathrm{d}\phi$$

$$J_{10} = \int_0^{\phi^*} \cos(\phi) I_0(\phi)\,\mathrm{d}\phi + \int_{\phi^*}^{\pi} \cos(\phi) I_0(\phi)\,\mathrm{d}\phi$$

and

$$J_0 = \int_0^{\phi^*} I_0(\phi)\,\mathrm{d}\phi + \int_{\phi^*}^{\pi} I_0(\phi)\,\mathrm{d}\phi$$

with

$$I_0(\phi) = 2\sqrt{(\alpha+\beta)}E(\pi/2, \sqrt{(2\beta/(\alpha+\beta))})$$

and

$$I_1(\phi) = \beta(F(\pi/2, \sqrt{(2\beta/(\alpha+\beta))})/\sqrt{(\alpha+\beta)} + (1/(3\beta^2\sqrt{(\alpha+\beta)}))((2\alpha^2+\beta^2) \times F(\pi/2, \sqrt{(2\beta/(\alpha+\beta))}) - 2\alpha(\alpha+\beta)E(\pi/2, \sqrt{(2\beta/(\alpha+\beta))})$$

and

(iii) $E > 4h$

$$J_1 = \int_0^{\pi} I_1(\phi)\,\mathrm{d}\phi \qquad J_{10} = \int_0^{\pi} \cos(\phi) I_0(\phi)\,\mathrm{d}\phi \qquad \text{and} \qquad J_0 = \int_0^{\pi} I_0(\phi)\,\mathrm{d}\phi.$$

The results for the conductivity are shown in figure 4. It was confirmed numerically that $J_1 = J_{10}$ in each regime. Given that $m^* \sim m_e$ for alkali metals providing one electron per atom to the wire, one would need a small $m^\dagger$ (or large h) for the conductivity to be approximately isotropic. In the case of Pb or Bi contributing 4 or 5 electrons, the conductivity will be more anisotropic than in the case where only one electron is contributed. In the regime where $h \sim 0.05$–0.25 eV, we see a relatively isotropic conductivity. Zeolites with a less dense set of columns for intercalating will have a more anisotropic conductivity. In this latter case, the tight-binding energy bands are very narrow, and a detailed microscopic calculation of the scattering processes may allow for an extra degree of anisotropy in τ and hence the conductivity, according to whether the scattering involves changes in the k-vector in the z or x, y directions.

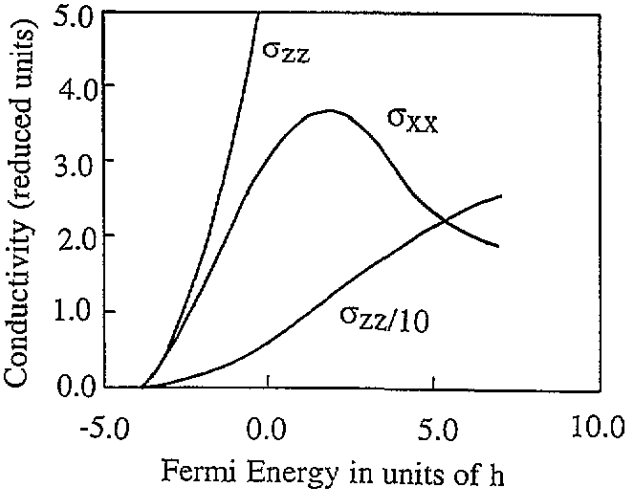

Figure 4. The two independent values of the conductivity as a function of the Fermi energy, (expressed in units of the parameter h) for the simple free-electron tight-binding band structure.

3. The tight-binding-nearly-free-electron model electronic structure

3.1. Density of states

A one band approximation as introduced in the last section cannot be used to describe the optical properties. Higher subbands based on the excited states of the cylinder and free-electron motion along the column will be too simple to account for optical properties, as in this case there is no absorption when light is polarized parallel to the column. We can remedy this with a nearly-free-electron model along the axis of the column. Such an extension to the model also allows us to account in an approximate way for the fact that the columns do not have a uniform cross section along their length — rather they widen out in the centre of the unit cell shown in figure 1 and narrow at the edges of the cell where the silicate cages link up. We assume a single weak periodic component to the potential seen by electrons in the direction of the column and we replace the z-component of the free-electron band structure $\hbar^2k_z^2/2m^*$ with the more complex nearly-free-electron (NFE) expression [13],

$$E_z(k_z) = (\hbar^2k_z^2/2m^* + \hbar^2(k_z - K)^2/2m^*)/2 \pm \sqrt{(((\hbar^2k_z^2/2m^* - \hbar^2(k_z - K)^2/2m^*)/2)^2 + V^2)} \tag{4}$$

where V and $K = 2\pi/d$ are the amplitude and wavenumber of the periodic potential. For reference below, the reduced units used below for these quantities are $\chi = V/(\hbar^2/2m^*d^2)$ and $\eta = h/(\hbar^2/2m^*d^2)$. The value of K is set by the crystal structure, but the amplitude V is another parameter (like h above), and is estimated below. There are two bands because of the $\pm$ factor, and optical absorption can now occur between these bands when light is polarized along the metal wire. The band structure is shown schematically in figure 5.

An alternative expression for the density of states, capable of handling the more complex $E(k_z)$, is obtained by performing the integrals in k_x and k_y in equation (1) and leaving the k_z integral to be done numerically. The relevant expression is (with $\zeta = k_zd$)

$$N(E) = (1/\pi^3d^3h)\int_0^{\pi} \mathrm{d}\zeta\, F(\pi/2, \sqrt{(1 - \Delta^2(\zeta)/16h^2)})$$

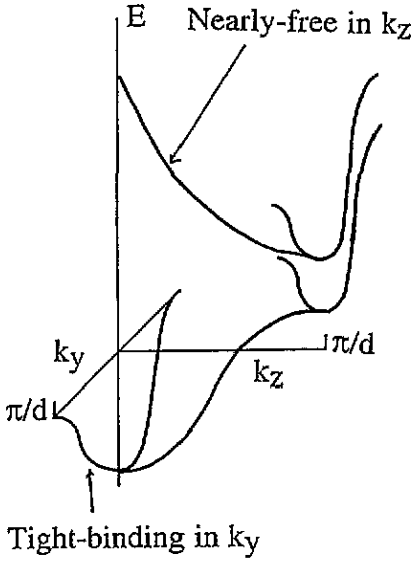

Figure 5. The schematic band structure in the tight-binding-nearly-free-electron model.

with

$$\Delta(\zeta) = E - (\hbar^2/2m^*d^2)((\zeta^2 + (\zeta - 2\pi)^2)/2 \pm \sqrt{((\zeta^2 - (\zeta - 2\pi)^2)/4 + \chi^2)})$$

where $\chi = V/(\hbar^2/2m^*d^2)$, and the integrand is zero if $|\Delta| > 4h$. In the limit of $\chi = 0$, the results coincide with those obtained in the previous section.

3.2. Results and estimates of band structure parameter values

In figure 6(a), the density of states is shown for the cases where $\eta = h/(\hbar^2/2m^*d^2) = 1$ (i.e. narrow bands in the k_x–k_y plane) and where $\chi = 0$ (i.e. no periodic potential, but a finite unit cell extent in the k_z direction), and $\chi = 10$ (a sizable periodic potential). The important point here is that there is an upper limit to the energy of the lowest band when $k_z = \pi/a$. This is shown explicitly in the case where $\chi = 10$. An estimate of the value of V can be obtained by equating to $2V$ the difference in ground-state energy of electrons in wide and narrow cylinders, whose radii correspond to the different parts of the unit cell. For the case of $a = 0.35$ nm above as the narrowest radius, and with $a = 0.5$ nm as the widest value, then $V = 0.15$ eV, and $\chi \sim 15$. In practice when $d = 2$ nm, $\hbar^2/2m^*d^2 = 9.2$ meV, so for moderately wide bands, $\eta \sim 10$, and the density of states for this case is plotted in figure 6(b). Now the density of states is essentially two-dimensional tight-binding-like, the amount of dispersion in the k_z direction being very small out to the first Brillouin zone boundary. This aspect of the NFE band structure greatly reduces the anisotropy of the system compared with that in the previous section. If $\eta > \pi^2/4$, there is more energy dispersion in the k_x–k_y plane than in the k_z direction in the lowest subband in the limit $\chi = 0$, and for $\chi > 0$, this range in η for this to occur is even wider.

3.3. Conductivity

The expression for the conductivity of the nearly-free-electron tight-binding approximation to the band structure is obtained numerically, as only one of the three integrals can be

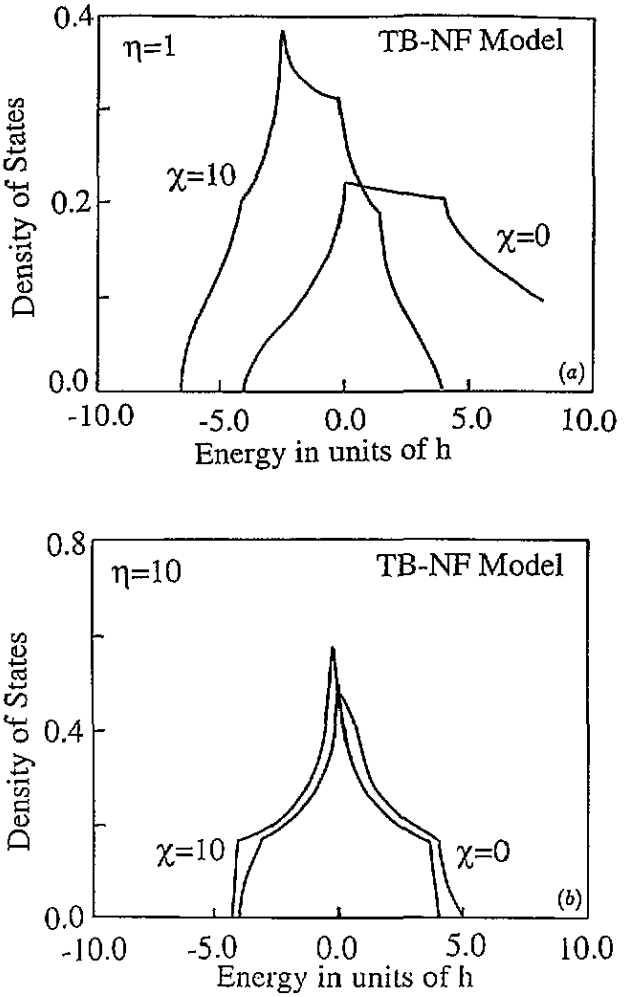

Figure 6. The density of states in energy (expressed in units of the parameter h) for the nearly-free-electron tight-binding band structure for two values of the amplitude of the periodic potential V, and two values of the relative dispersion in the directions parallel and perpendicular to the columns.

performed analytically. The results, for the cases $\chi = V/(\hbar^2/2m^*d^2) = 0$ and $\chi = 10$ and for $\eta = h/(\hbar^2/2m^*d^2) = 1$ and $\eta = 10$ are shown in figures 7(a) and 7(b). In all cases the conductivity is rather less anisotropic than in figure 4, reaching a maximum value of ~ 2, once there is about one electron per unit cell. The anisotropy always favours transport in the z-direction.

In these diagrams, we can use the Fermi energy as a variable that correlates with the relative density of intercalated species, on the assumption that each intercalated atom gives up a fixed number of electrons irrespective of the density of the intercalate. If this intercalation density exceeds two atoms per silicate formula unit, the lowest of the subbands is filled. (Note in the case where the density is just less than two per formula unit is may be possible to obtain the analogue of hole transport in semiconductors, with the changing sign of the effective masses.) We have repeated the calculations of the density of states and

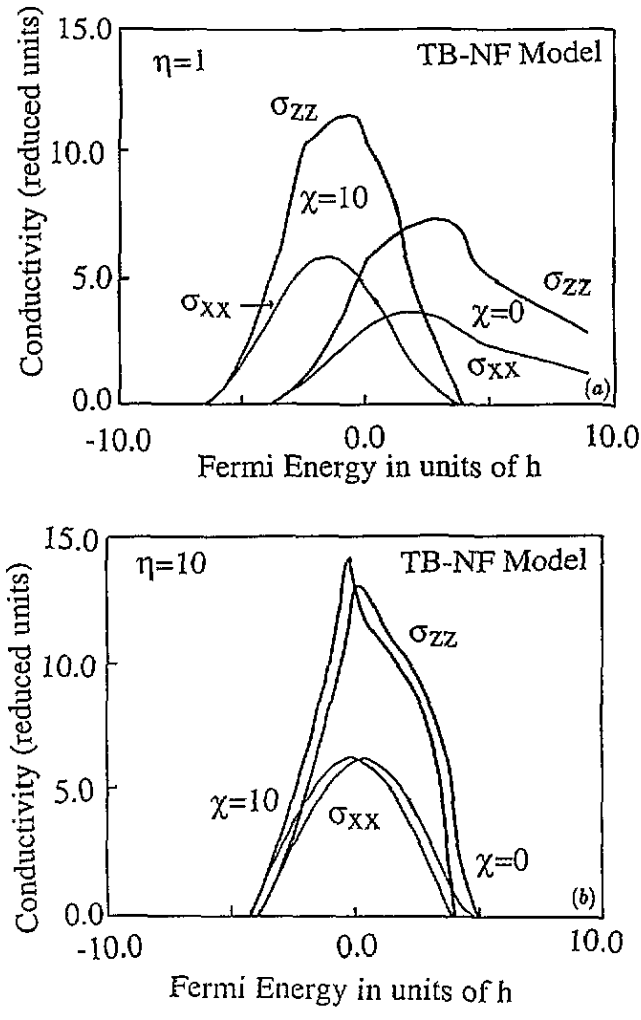

Figure 7. The two independent values of the conductivity as a function of the Fermi energy, (expressed in units of the parameter h) for the nearly-free-electron tight-binding band structure for two values of the amplitude of the periodic potential V, and two values of the relative dispersion in the directions parallel and perpendicular to the columns.

conductivity for the second subband (the + sign in equation (4) above), for the same values of the parameters used in figures 6 and 7. This second band is much wider in energy for $\eta = 1$, but not appreciably so when $\eta = 10$. Again the conductivity is not very anisotropic under any circumstances.

3.4. Optical properties

Once we have two bands and a Fermi energy that lies in the range of the lower band, we can calculate the optical absorption, as a function of the photon energy $\hbar\omega$. In practice we have to calculate the detailed matrix element between initial and final state wavefunctions, but here we make an initial approximation that this matrix element is constant. In this restricted regime, the optical absorption is proportional to the optical density of states, $J(\hbar\omega)$, i.e. the

number of pairs of states separated in energy by the photon energy and weighted by the condition that the initial state is occupied and the final state empty,

$$J(\hbar\omega) = \int \mathrm{d}k\, f(E_1(k))[1 - f(E_2(k))]\delta(E_2(k) - E_1(k) - \hbar\omega)(4\pi^3). \quad (5)$$

In the relatively simple case where the Fermi energy is in a gap between a filled lower band and an empty upper band (as when V is strong enough to open an absolute band gap and there are two electrons per unit cell), the above expression simplifies (when the tight binding parameter is the same in both bands) to

$$J(\hbar\omega) = \begin{cases} [1/(\pi^2 a^3)]\hbar\omega/\sqrt{((\hbar\omega)^2 - 4V^2)} & \text{for } 2|V| < \hbar\omega < \sim \hbar^2K^2/2m^* \\ 0 & \text{otherwise} \end{cases}$$

which is broad and featureless within the range of energies for which it is non-zero. We have calculated $J(\hbar\omega)$, assuming that the upper tight binding band is described by a modified interaction parameter h', for a range of positions of the Fermi energy in the lower band, and the same sets of parameters as above ($\chi = 0, 10$, $\eta = 1, 10$). Typical results are shown in figure 8. Again the lack of features in the computed results makes experimental results difficult to interpret using this approach, as the width of any optical absorption feature is a complex interaction of tight-binding parameters h and h', the amplitude and wavelength (χ and η) of the periodic potential.

The full expression [14] for the optical conductivity tensor σ involves the optical matrix element between initial and final states $\Psi_i(k)$, $\Psi_f(k)$

$$|\langle\Psi_f|\varepsilon \cdot \nabla|\Psi_i\rangle\langle\Psi_i|\varepsilon \cdot \nabla|\Psi_f\rangle|$$

as a factor within the integral expression in equation (5), with ε the polarization vector of the light. The matrix element distinguishes the nature of the wavefunction along the axis of the columns which determines σ_{zz} and radially within each column which determines σ_{xx}. Any anisotropy in the diagonal optical conductivity can then be used to extract V for the σ_{zz} component and a convolution of tight-binding parameters from the $\sigma_{xx} = \sigma_{yy}$ components. Such an exercise is better undertaken in the detailed interpretation of specific experimental results.

4. Discussion

The modest anisotropy of electrical and optical properties obtained within the simple models of the electronic structure of ion-intercalated zeolites suggests that the interactions between wires are too great. Only if the tight-binding bands are only a few millivolts wide is there appreciable anisotropy. Zeolites would need to have $\geqslant 3$ nm separation between adjacent columns rather than the ~ 2 nm used so far. This would make it easier to ensure that the tight-binding bands are either full or empty while having a part filled band in the k_z direction, thus limiting the conductivity transverse to the wires, and enhancing the anisotropy of both the electrical and optical conductivity. This is the regime of η large. The simple one-electron theory tends to break down with very narrow bands, with modifications to the transport properties caused by electron-electron correlations. A dense bundle of one-dimensional wires then becomes even more difficult to realise.

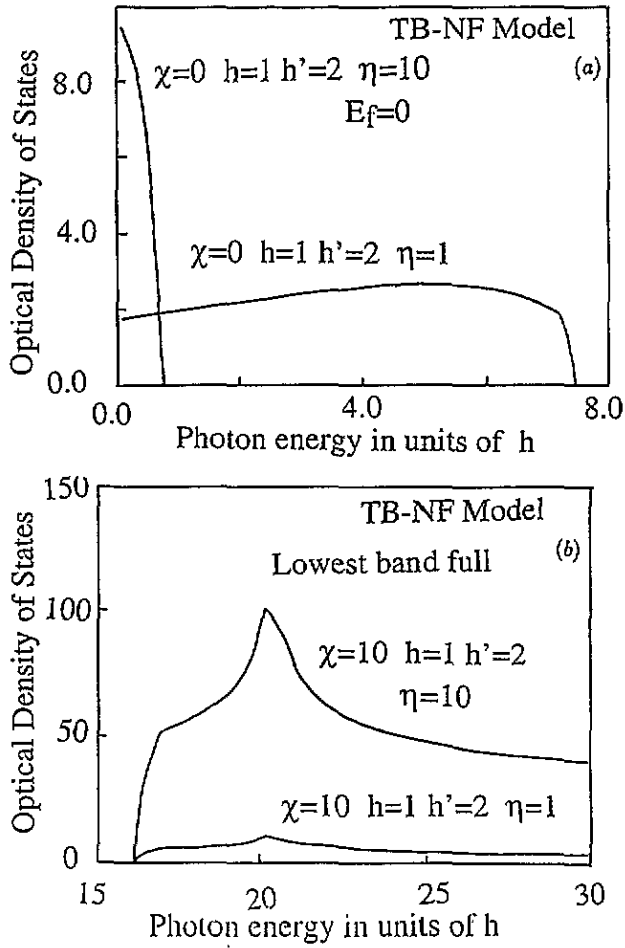

Figure 8. The joint density of states as a function of photon energy, assuming a constant matrix element for the optical absorption in the model band structure, calculated for specific sets of band structure parameters. Note that h (h') are the tight-binding parameters for the first (second) bands.

The range of results shows the extent to which the density of intercalated metals can be used to alter the electronic and optical properties of the zeolites. The simple model here assumes a constant and uniform electron density from the intercalated atoms as a variable. In practice this can be difficult to achieve, since a given unit cell will have discrete number of intercalate atoms, and averaging will need to be done over relatively large volumes. A very high integrity is assumed of the metal wires once formed, and this may be difficult to achieve in practice. If, however, initial optical and transport measurements give promising results in terms of anisotropy, a more elaborate theory of electronic structure may be appropriate. Such a theory would also have to address further issues such as Peierls distortions and related instabilities in Q1D systems embedded in a 3D matrix.

Appendix. A dense bundle of Q1D wires

The resistance of a piece of copper of 3 μm square cross section and 10 μm length at 77 K

is 0.017 Ω. Below 77 K, the resistance of ultra-pure copper drops by several orders of magnitude, while by room temperature the resistance rises to ~ 0.14 Ω. Consider a set of $10^3 \times 10^3$ Q1D wires centred 3 nm apart on a square lattice in a plane perpendicular to the wire axes, and each wire having one ballistic electron channel [15]. The resistance of each channel at low temperature is $h/(2e^2)$, and the overall resistance of the array is 0.012 Ω. The temperature dependence of this resistance is not well characterized, but is small at low temperature [16], and the ballistic electron effects have been seen up to nearly 200 K [17] in suitable systems, again with a modest temperature dependence. It is argued that a suitable bundle of Q1D wires, such as metal-intercalated zeolites, might share this property to even higher temperatures. A combination of low resistance and low temperature variation of the resistance is attractive in device design.

References

[1] Weisbuch C and Vinter B 1991 *Quantum Semiconductor Structures* (New York: Academic)

[2] Kelly M J 1993 *Int J. Electron.* **75** 27–40

[3] Dyer A 1988 *An Introduction to Zeolite Molecular Sieves* (New York: Wiley)

[4] Romanov S 1993 *J. Phys.: Condens. Matter* **5** 1081–90

[5] Anderson P A, Armstrong A R and Edwards P P 1994 *Angew. Chem. Int. Edn Engl.* **33** 641–3

[6] Terasaki O, Yamazaki K, Thomas J M, Ohsuna T, Watanabe D, Sanders J V and Barry J C 1987 *Nature* **330** 58–60

Nozue Y, Kodaira T, Terasaki O, Yamazaki K, Goto T, Watanabe D and Thomas J M 1990 *J. Phys.: Condens. Matter* **2** 5209–17

[7] Kelly M J 1985 *J. Phys. C: Solid State Phys.* **16** 6341–53

[8] Tsubaki K, Honda T, Saito H and Fukui T 1992 *Surf. Sci.* **267** 270–3

[9] Abramowitz M and Stegun I A 1965 *Handbook of Mathematical Functions* (New York: Dover)

[10] Gradshteyn I S and Ryzhik I M 1965 *Table of Integrals Series and Products* (New York: Academic)

[11] The NAG Fortan Library, NAG Ltd (Oxford)

[12] Note that one has to be careful in matching the different nomenclature for elliptic functions between the three preceding references.

[13] Ashcroft N W and Mermin N D 1976 *Solid State Physics* (New York: Holt, Rinehardt and Winstone)

[14] Kelly M J and Ashcroft N W 1971 *Phys. Rev.* B **8** 2445–8

[15] van Wees B J, van Houten H, Beenakker C W J, Williamson J G, Kouvenhoven L P, van der Marel D and Foxon C T 1988 *Phys. Rev. Lett.* **60** 848–50

Wharam D A, Thornton T J, Newbury R, Pepper M, Ahmed H, Frost J E F, Hasko D G, Peacock D C, Ritchie D A and Jones G A C 1988 *J. Phys. C: Solid State Phys.* **21** L209–13

[16] van Houten H, Beenakker C W J and van Wees B J 1992 *Semimetals and Semiconductors* vol 35, ed M Reed, R K Willardson, A C Beer and E R Weber (New York: Academic) pp 9–112

[17] Hajto J, Owen A E, Snell A J, Le Comber P G and Rose M J 1991 *Phil. Mag.* B **63** 349–69